

# Probing Non-perturbative Supersymmetry Breaking through Lattice Path Integrals

Navdeep Singh Dhindsa<sup>1,\*</sup> and Anosh Joseph<sup>1,†</sup>

<sup>1</sup>*Department of Physical Sciences, Indian Institute of Science Education and Research (IISER) Mohali, Knowledge City, Sector 81, SAS Nagar, Punjab 140306, India*

(Dated: December 1, 2020)

## Abstract

We investigate non-perturbative supersymmetry breaking in various models of quantum mechanics, including  $\mathcal{PT}$ -symmetric models, using lattice path integrals. These theories are discretized on a temporal Euclidean lattice with periodic or anti-periodic boundary conditions. Hamiltonian Monte Carlo algorithm is used to update the field configurations to their equilibrium values. The ratios of fermionic and bosonic mass gaps, and Ward identities are used as tools for probing supersymmetry breaking. Our simulations suggest that non-perturbative supersymmetry breaking is absent in quantum mechanics models exhibiting  $\mathcal{PT}$ -symmetry.

arXiv:2011.08109v2 [hep-lat] 30 Nov 2020

---

\* [navdeep.s.dhindsa@gmail.com](mailto:navdeep.s.dhindsa@gmail.com)

† [anoshjoseph@iisermohali.ac.in](mailto:anoshjoseph@iisermohali.ac.in)

## CONTENTS

I. Introduction	2
II. Supersymmetric Quantum Mechanics	3
A. Continuum Theory	3
B. Lattice Theory	4
III. Model with Various Superpotentials	5
A. Even-Degree Superpotential	5
1. Correlation Functions	5
2. Ward Identities	8
B. Odd-Degree Superpotential	10
1. Periodic Boundary Conditions	10
2. Anti-periodic Boundary Conditions	12
C. Scarf I Superpotential	17
D. Models with $\mathcal{PT}$ -Symmetry	17
IV. Conclusions	20
V. Acknowledgements	22
A. Continuum Theory Calculations	22
References	23

## I. INTRODUCTION

Supersymmetric quantum mechanics can be used as a test bed to illustrate several properties of systems containing bosons and fermions. The idea of dynamical supersymmetry (SUSY) breaking has been studied extensively in the literature since Witten's seminal work [1]. These investigations range from studying the properties of supersymmetric quantum mechanics to supersymmetric gauge theories in various dimensions [2–11]. In this work, we investigate non-perturbative SUSY breaking in various quantum mechanics models by regularizing them on a Euclidean lattice. The importance of supersymmetric quantum mechanics models can also be justified from the fact that they have been the subject of thorough investigations in the context of various physical systems over the past few decades. (See Ref. [12] for a review.) Supersymmetric quantum mechanics models, with quartic superpotential, have been simulated on the lattice over the past ten years or so with promising results - see Refs. [13–19]. In this work, we started with the quantum mechanics model with a quartic superpotential, in order to verify the existing simulation results in the literature, and then we moved on to simulating the interesting case of  $\mathcal{PT}$ -symmetric quantum mechanics. Although the Euclidean action of the  $\mathcal{PT}$ -symmetric quantum mechanics is complex, for an arbitrary value of the parameter  $\delta$  appearing in the potential, we were able to simulate a subset of it; for  $\delta = 0, 2, 4$ , where the action becomes real. Our simulations indicate that these models do not exhibit dynamical SUSY breaking. All the models discussed in this paper were

simulated using lattice regularized versions of the Euclidean path integrals, with the Hamiltonian Monte Carlo (HMC) algorithm as the tool to update the field configurations in simulation time. For a general  $\mathcal{PT}$ -symmetric model with complex action, we can use complex Langevin dynamics to explore the nature of SUSY breaking. See Ref. [20] for more details.

The paper is organized as follows. In Sec. II we briefly discuss supersymmetric quantum mechanics in the continuum and also on the lattice. In Sec. III we study the model with various superpotentials. They include polynomial type of potentials with degrees four and five (in Secs. III A and III B), Scarf I potential (in Sec. III C) and finally the  $\mathcal{PT}$ -symmetric superpotential (in Sec. III D). We provide conclusions in Sec. IV. In Appendix A some continuum theory calculations are provided.

## II. SUPERSYMMETRIC QUANTUM MECHANICS

### A. Continuum Theory

The Euclidean action of supersymmetric quantum mechanics has the following off-shell form

$$S = \int d\tau \left( -\frac{1}{2} \phi \partial_\tau^2 \phi + \bar{\psi} \partial_\tau \psi - \frac{1}{2} B^2 + \bar{\psi} W''(\phi) \psi - B W'(\phi) \right), \quad (2.1)$$

where  $\phi$  and  $B$  are real bosonic fields,  $\bar{\psi}$  and  $\psi$  are fermionic fields. The fields depend only on the Euclidean time variable  $\tau$ , and  $\partial_\tau$  is the derivative with respect to  $\tau$ . The object  $W(\phi)$  is a yet unspecified function, called the superpotential, and the primes denote its derivatives with respect to  $\phi$ .

The above action is invariant under two supercharges  $Q$  and  $\bar{Q}$ . They obey the following algebra

$$\begin{aligned} \{Q, Q\} &= 0, \\ \{\bar{Q}, \bar{Q}\} &= 0, \\ \{Q, \bar{Q}\} &= 2\partial_\tau. \end{aligned} \quad (2.2)$$

We can integrate out the auxiliary field  $B$  from the action using its equation of motion

$$B = -W'(\phi). \quad (2.3)$$

Then the on-shell action takes the form

$$S = \int d\tau \left( -\frac{1}{2} \phi \partial_\tau^2 \phi + \bar{\psi} \partial_\tau \psi + \bar{\psi} W''(\phi) \psi + \frac{1}{2} [W'(\phi)]^2 \right). \quad (2.4)$$

The supercharges  $Q$  and  $\bar{Q}$  act on the fields in the following way

$$Q\phi = \bar{\psi}, \quad Q\psi = -\partial_\tau \phi + W', \quad Q\bar{\psi} = 0, \quad (2.5)$$

and

$$\bar{Q}\phi = -\psi, \quad \bar{Q}\psi = 0, \quad \bar{Q}\bar{\psi} = \partial_\tau \phi + W'. \quad (2.6)$$

## B. Lattice Theory

We are interested in investigating non-perturbative SUSY breaking in the model. For that we will consider the path integral quantization of the model, discretized on a one-dimensional Euclidean lattice. The lattice has  $T$  number of equally spaced sites with the lattice spacing  $a = T^{-1}$ .

The lattice regularized action has the form

$$S = \sum_{ij} \left( -\frac{1}{2} \phi_i D_{ij}^2 \phi_j + \bar{\psi}_i M_{ij} \psi_j \right) + \frac{1}{2} \sum_i W_i' W_i', \quad (2.7)$$

where the indices  $i$  and  $j$  represent the lattice sites and they run from 0 to  $T - 1$ . The fermion operator is denoted as  $M$  and the elements of this matrix,  $M_{ij}$ , connect the sites  $i$  and  $j$ . The superpotential at site  $i$  is denoted by  $W_i$ .

It is well known that for supersymmetric theories on a lattice the presence of fermion doublers breaks SUSY. We could include a Wilson-mass term in the model to remove the doublers [21] and to get the expected target theory in the continuum. The Wilson mass matrix  $K_{ij}$  has the following form

$$K_{ij} = m \delta_{ij} - \frac{1}{2} (\delta_{i,j+1} + \delta_{i,j-1} - 2\delta_{ij}). \quad (2.8)$$

Upon defining  $W_{ij}''$  as

$$W_{ij}'' \equiv K_{ij} + W_i' \delta_{ij}, \quad (2.9)$$

and the symmetric difference operator

$$D_{ij} \equiv \frac{1}{2} (\delta_{j,i+1} - \delta_{j,i-1}), \quad (2.10)$$

we can express the elements of the fermion matrix as

$$M_{ij} = D_{ij} + W_{ij}''. \quad (2.11)$$

In order to simulate the fermionic sector of the theory we replace the fermions by pseudo-fermions  $\chi$  [22]. Then the action in Eq. (2.7) takes the form

$$S = \sum_{ij} \left( -\frac{1}{2} \phi_i D_{ij}^2 \phi_j + \chi_i (M^T M)_{ij}^{-1} \chi_j \right) + \frac{1}{2} \sum_i W_i' W_i'. \quad (2.12)$$

Our goal is to study the non-perturbative physics of this theory using an appropriate algorithm that implements the theory on a lattice. We use an algorithm that is relatively more efficient, which is known as the Hybrid Monte Carlo (HMC) algorithm [23, 24]. HMC algorithm contains a deterministic part (molecular dynamics) and a non-deterministic part (Metropolis test). As part of this algorithm we take  $p$  and  $\pi$  as the momenta conjugate to the fields  $\phi$  and  $\chi$ , respectively. Then the Hamiltonian of the system takes the form

$$H = \left[ \sum_{ij} \left( -\frac{1}{2} \phi_i D_{ij}^2 \phi_j + \chi_i (M^T M)_{ij}^{-1} \chi_j \right) + \frac{1}{2} \sum_i W_i' W_i' \right] + \frac{1}{2} \sum_i (p_i^2 + \pi_i^2). \quad (2.13)$$

This Hamiltonian is then evolved using a discretized version of Hamilton's equations, in a fictitious time  $\tau$ , using a small step size  $\epsilon$ . This is the molecular dynamics part of the algorithm. At the end of the evolution we get a new hamiltonian  $H'$ . We then accept or reject  $H'$  using the non-deterministic part of the algorithm.

### III. MODEL WITH VARIOUS SUPERPOTENTIALS

#### A. Even-Degree Superpotential

Let us consider the superpotential

$$W(\phi) = \frac{1}{2}m\phi^2 + \frac{1}{4}g\phi^4, \quad (3.1)$$

where  $m$  is the mass and  $g$  is the coupling constant. In Ref. [13] it was shown, using Monte Carlo simulations, that supersymmetry is preserved in this model. As a cross-check we will reproduce the results given in Ref. [13].

The bosonic action takes the following form on the lattice

$$S_B = \frac{1}{2} \sum_{ij} (-\phi_i D_{ij}^2 \phi_j) + \frac{1}{2} \sum_i W'_i W'_i. \quad (3.2)$$

Upon introducing the symmetric difference operator, as defined in Eq. (2.10), we get

$$S_B = \sum_i \left[ -\frac{1}{8} (\phi_i \phi_{i+2} + \phi_i \phi_{i-2} - 2\phi_i^2) + \frac{1}{2} W'_i W'_i \right]. \quad (3.3)$$

We also have

$$\begin{aligned} W'_i &= \sum_j K_{ij} \phi_j + g\phi_i^3 \\ &= m\phi_i + \phi_i - \frac{1}{2} (\phi_{i-1} + \phi_{i+1}) + g\phi_i^3. \end{aligned} \quad (3.4)$$

The fermion matrix takes the form

$$M_{ij} = (1 + m + 3g\phi_i^2) \delta_{ij} - \delta_{i,j+1}. \quad (3.5)$$

In the simulations we used the following dimensionless variables:  $m = m_{\text{phys}}a$ ,  $g = g_{\text{phys}}a^2$  and  $\phi = \phi_{\text{phys}}a^{-1/2}$ .

In Fig. 1 we show the Monte Carlo time history of the lattice action on a  $T = 8$  lattice. The simulation results clearly show that the average value fluctuate around 8, which is what we expect for the model, i.e.,  $\langle S \rangle = T$  [25].

#### 1. Correlation Functions

The bosonic and fermionic correlation functions can be used to extract the mass gaps. We have the bosonic correlator

$$G_{ij}^B \equiv \langle \phi_i \phi_j \rangle. \quad (3.6)$$

In the simulations we consider a variant of this

$$G_{0,\text{site}}^B = \langle \phi_0 \phi_{\text{site}} \rangle. \quad (3.7)$$

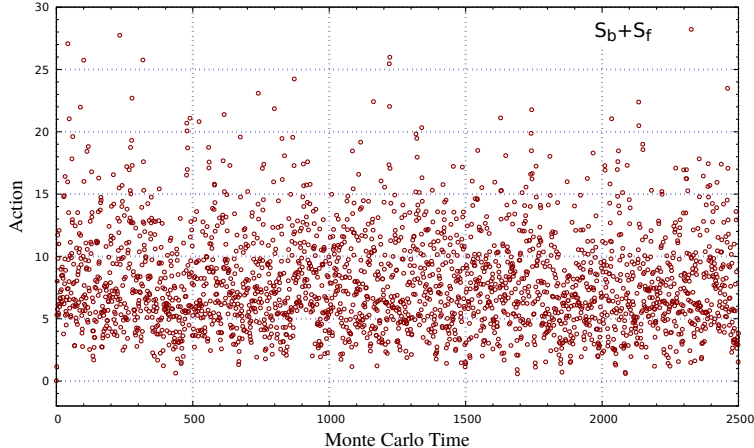


FIG. 1: Monte Carlo time history of the action  $\langle S \rangle$  on a  $T = 8$  lattice for the first 250,000 Monte Carlo steps with the gap of 100 steps between the measurements. We expect  $\langle S \rangle = 8$ . The simulations give  $\langle S \rangle = 8.0525(1138)$ .

The fermionic correlator has the form

$$G_{ij}^F = \langle \bar{\psi}_i \psi_j \rangle. \quad (3.8)$$

In the case of pseudo-fermions, its estimator can be written as [13]

$$G_{ij}^F = \langle s_j M_{ik} s_k \rangle. \quad (3.9)$$

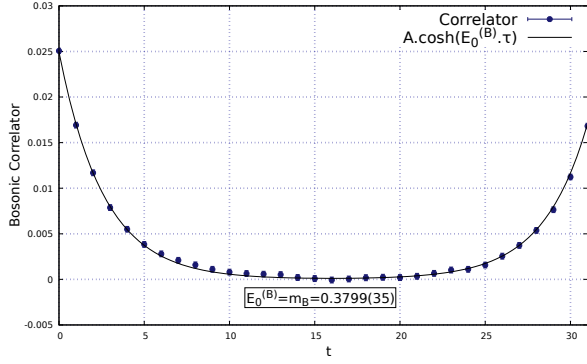
We will consider its variant

$$G_{0,\text{site}}^F = \langle s_{\text{site}} (Ms)_0 \rangle \quad (3.10)$$

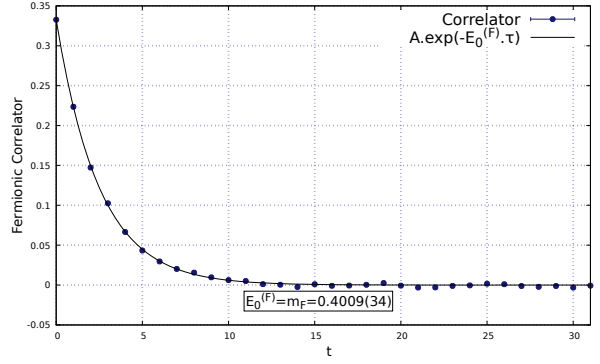
in the simulations.

We performed the simulations of this model for  $T = 8, 16, 32, 64$  and  $128$ . In Fig. 2 we show the simulation results for the bosonic and fermionic correlators for parameters  $m = 10$  and  $g = 100$  for  $T = 32$ .

We can extract the mass gap from the correlator by fitting it to the form  $A \cosh(E_0 \tau)$  and  $A e^{-E_0 \tau}$  for bosonic and fermionic correlators, respectively. The mass gap is defined as  $E_0^{\text{phys}} = m_{\text{phys}} = E_0/a = E_0 T$ . In Table I we provide the extracted values of the mass gaps (bosonic and fermionic) after fitting the correlators. Our simulations show that the ratio of extracted mass gaps is nearly equal to 1 for simulations with different number of lattice sites. This indicates that SUSY is not broken in this model, and this is in close agreement with the results of Refs. [13, 14, 17]. The expectation values of the action are given in Table II. The plot of normalized action to lattice sites is shown in Fig. 3. In Fig. 4 we show the plot of the physical mass against the lattice spacing  $a$  for both bosons and fermions along with the ratios of these masses.



(a) Bosonic correlator.



(b) Fermionic correlator.

FIG. 2: The bosonic and fermionic correlators on the lattice for the model with degree-four superpotential. We used  $T = 32$  with  $m = 10$  and  $g = 100$ . The solid curves represent fits to the data.

$T$	$a = T^{-1}$	$E_0^{(B)\text{phys}} \equiv m_{b(\text{phys})}$	$E_0^{(F)\text{phys}} \equiv m_{f(\text{phys})}$	Mass Ratio = $\frac{m_{b(\text{phys})}}{m_{f(\text{phys})}}$
8	0.125	8.0644(2640)	8.4159(1304)	0.9582(462)
16	0.0625	10.3366(2384)	10.7571(1278)	0.9609(336)
32	0.03125	12.1568(1120)	12.8288(1088)	0.9476(168)
64	0.015625	13.7082(4416)	14.9600(1798)	0.9163(405)
128	0.0078125	16.5056(6298)	15.5136(2522)	1.0639(579)

TABLE I: The bosonic and fermionic mass gaps and their ratios for degree-four superpotential with different number of lattice sites  $T$ . The parameters used are  $m = 10$  and  $g = 100$ .

$T$	$\langle S \rangle$	$\frac{\langle S \rangle}{T}$
8	8.0525(1138)	1.0066(142)
16	16.0307(293)	1.0019(18)
32	32.0407(529)	1.0013(16)
64	63.9786(1061)	0.9997(17)
128	127.9530(2489)	0.9996(19)

TABLE II: The expectation values of the action for degree-four superpotential. The parameters used are  $m = 10$  and  $g = 100$ . The exact value is  $\langle S \rangle / T = 1$  for a theory with unbroken SUSY.

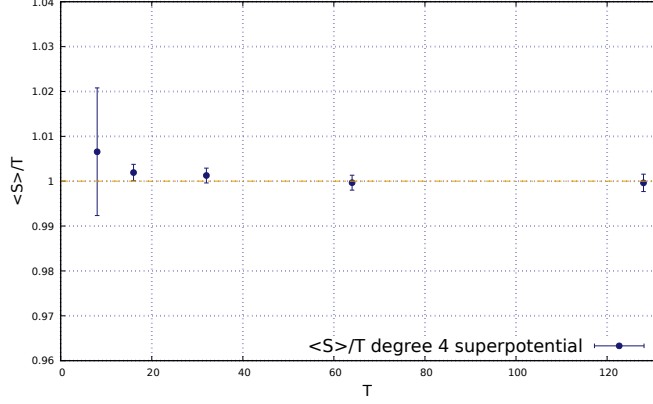


FIG. 3: The normalized action for degree-four superpotential. The parameters used are  $m = 10$  and  $g = 100$ . The dashed horizontal line indicates the exact value of  $\langle S \rangle / T$ . Our simulations suggest that SUSY is unbroken in this model.

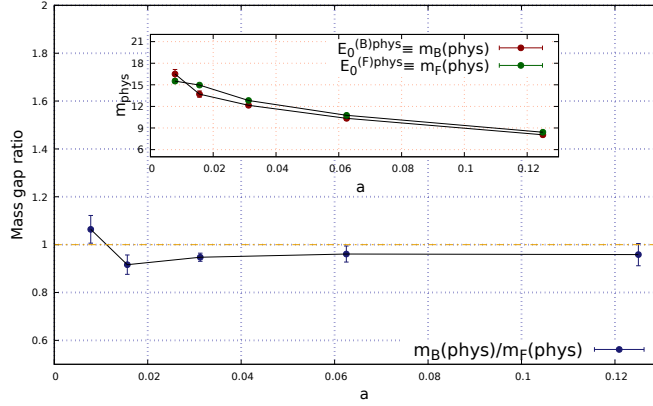


FIG. 4: The mass gap ratio against lattice spacing  $a$  for degree-four superpotential. The parameters used are  $m = 10$  and  $g = 100$ . The data indicate that SUSY is preserved in this model. In the box the plot of  $m_{\text{phys}}$  against  $a$  is shown.

## 2. Ward Identities

We can derive a Ward identity by rewriting the expectation value of an observable say,  $\mathcal{O}(\phi)$  in the path integral formulation by considering the infinitesimal transformations  $\phi \rightarrow \phi' = \phi + \delta\phi$  with  $\mathcal{D}\phi' = \mathcal{D}\phi$ . Under these transformations  $\langle \mathcal{O} \rangle$  becomes

$$\begin{aligned}
 \langle \mathcal{O} \rangle &= \frac{1}{Z} \int \mathcal{D}\phi' \mathcal{O}(\phi') e^{-S(\phi')}, \\
 &= \frac{1}{Z} \int \mathcal{D}\phi [\mathcal{O}(\phi) + \delta\mathcal{O}(\phi) e^{-S(\phi+\delta\phi)}], \\
 &= \frac{1}{Z} \int \mathcal{D}\phi \mathcal{O}(\phi) e^{-S(\phi)} [1 - \delta S(\phi)] + \frac{1}{Z} \int \mathcal{D}\phi \delta\mathcal{O}(\phi) e^{-S(\phi)} [1 - \delta S(\phi)]. \quad (3.11)
 \end{aligned}$$

In the above equations we expanded the exponential up to first order. Now, upon neglecting



the  $\delta S \delta \mathcal{O}$  term we get

$$\langle \mathcal{O} \rangle = \frac{1}{Z} \int \mathcal{D}\phi \mathcal{O}(\phi) e^{-S(\phi)} [1 - \delta S(\phi)] + \frac{1}{Z} \int \mathcal{D}\phi \delta \mathcal{O}(\phi) e^{-S(\phi)}, \quad (3.12)$$

$$= \langle \mathcal{O} \rangle - \frac{1}{Z} \int \mathcal{D}\phi \mathcal{O}(\phi) \delta S(\phi) e^{-S(\phi)} + \frac{1}{Z} \int \mathcal{D}\phi \delta \mathcal{O}(\phi) e^{-S(\phi)}. \quad (3.13)$$

Thus we are left with

$$\langle \mathcal{O} \delta S \rangle = \langle \delta \mathcal{O} \rangle. \quad (3.14)$$

Since the action is invariant under the infinitesimal transformation  $\delta$ , we must have

$$\langle \delta \mathcal{O} \rangle = 0. \quad (3.15)$$

Let us consider the following two supersymmetry transformations

$$\begin{aligned} \delta_1 \phi_i &= \bar{\psi}_i \epsilon, & \delta_2 \phi_i &= \bar{\epsilon} \psi_i, \\ \delta_1 \psi_i &= -(D_{ik} \phi_k - W'_i) \epsilon, & \delta_2 \psi_i &= 0, \\ \delta_1 \bar{\psi}_i &= 0, & \delta_2 \bar{\psi}_i &= \bar{\epsilon} (D_{ik} \phi_k + W'_i), \end{aligned} \quad (3.16)$$

where  $\epsilon$  and  $\bar{\epsilon}$  denote the infinitesimal Grassmann odd variables that generate supersymmetry.

Let us take  $\mathcal{O} = \phi_i \bar{\psi}_j$ . Upon using the transformation  $\delta_2$  in Eq. (3.15) we get

$$\langle \delta_2 \mathcal{O} \rangle = 0 \quad \implies \quad \langle (\phi_i \cdot \delta_2 \bar{\psi}_j + \delta_2 \phi_i \cdot \bar{\psi}_j) \rangle = 0. \quad (3.17)$$

Expanding the terms we have

$$\langle (\phi_i \cdot \bar{\epsilon} (D_{jk} \phi_k + W'_j) + \bar{\epsilon} \psi_i \cdot \bar{\psi}_j) \rangle = 0.$$

Upon simplification we arrive at

$$\langle \phi_i (D_{jk} \phi_k + W'_j) - \bar{\psi}_j \psi_i \rangle = 0. \quad (3.18)$$

We note that when we apply the transformation  $\delta_1$  on the same observable  $\phi_i \bar{\psi}_j$  our result vanishes trivially. Taking  $\mathcal{O} = \phi_i \psi_j$  and applying the transformation  $\delta_1$  on it, we get the following from Eq. (3.15)

$$\begin{aligned} \langle \delta_1 \mathcal{O} \rangle = 0 \quad \implies \quad & \langle (\phi_i \cdot \delta_1 \psi_j + \delta_1 \phi_i \cdot \psi_j) \rangle = 0 \\ & \langle (-\phi_i \cdot (D_{jk} \phi_k - W'_j) \epsilon + \bar{\psi}_i \epsilon \cdot \psi_j) \rangle = 0. \end{aligned} \quad (3.19)$$

Upon simplification this becomes

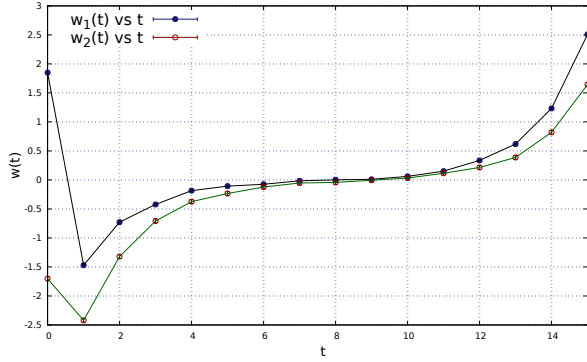
$$\langle \phi_i (D_{jk} \phi_k - W'_j) + \bar{\psi}_i \psi_j \rangle = 0. \quad (3.20)$$

Eqs. (3.18) and (3.20) are our Ward identities. We will check these identities through the following two quantities

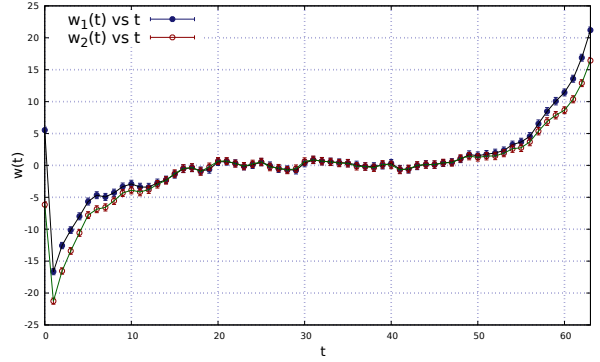
$$w_1(t) \equiv \langle \phi_i (D_{jk} \phi_k + W'_j) \rangle - G_{ji}^F, \quad (3.21)$$

$$w_2(t) \equiv \langle \phi_i (D_{jk} \phi_k - W'_j) \rangle + G_{ij}^F. \quad (3.22)$$

If SUSY is preserved in the model these quantities should fluctuate around 0, at least in the middle region of the lattice. We show the simulation results for Ward identities in Fig. 5. These results, along with the extracted mass-gap ratios, indicate that SUSY is preserved in this model.



(a) Ward identities on a  $T = 16$  lattice.



(b) Ward identities on a  $T = 64$  lattice.

FIG. 5: Ward identities for the model with degree-four superpotential. The simulations were performed on  $T = 16$  and  $T = 64$  lattices. The parameters used were  $m = 10$  and  $g = 100$ . The simulations show that SUSY is preserved in this model.

## B. Odd-Degree Superpotential

Let us consider a model with degree-five superpotential. Supersymmetry is spontaneously broken in this model [5]. So we should expect a non-vanishing ground state energy, in addition to the bosonic and fermionic excitations having different energies.

According to our lattice prescription the derivative of the superpotential for this model takes the following form

$$\begin{aligned}
 W'_i &= \sum_j K_{ij} \phi_j + g \phi_i^4 \\
 &= m \phi_i + \phi_i - \frac{1}{2} (\phi_{i-1} + \phi_{i+1}) + g \phi_i^4.
 \end{aligned} \tag{3.23}$$

### 1. Periodic Boundary Conditions

The dimensionless parameters of the lattice version of the model are  $m = m_{\text{phys}} a$ ,  $g = g_{\text{phys}} a^{5/2}$  and  $\phi = \phi_{\text{phys}} a^{-1/2}$ . We simulated this model with the parameters  $m = 10$  and  $g = 100$ . Again, by fitting the correlators we extracted the mass gaps for both the bosons and fermions. The results are shown in Table III.

The plot of the mass-gap ratios against  $a$  along with the extracted bosonic and fermionic mass gaps is given in Fig. 6. In Fig. 7 we show the Ward identities of the model.

$T$	$a = T^{-1}$	$E_0^{(B)\text{phys}} \equiv m_{b(\text{phys})}$	$E_0^{(F)\text{phys}} \equiv m_{f(\text{phys})}$	Mass Ratio = $\frac{m_{b(\text{phys})}}{m_{f(\text{phys})}}$
8	0.125	8.2510(6238)	6.4876(2021)	1.2718(1358)
16	0.0625	9.7789(7698)	7.6654(182)	1.2757(1034)
32	0.03125	9.6768(4237)	7.8074(1181)	1.2394(734)
64	0.015625	10.8865(4583)	7.7555(2419)	1.4037(1029)

TABLE III: The bosonic and fermionic mass gaps and their ratios for degree-five superpotential for various lattice sites  $T$ . The simulation parameters used were  $m = 10$  and  $g = 100$ . The data indicate that SUSY is broken in this model.

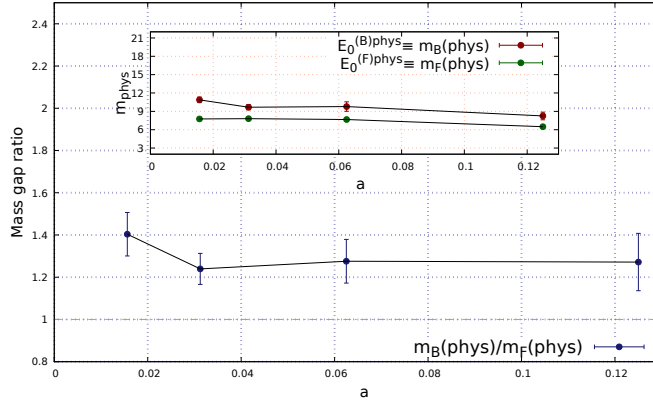
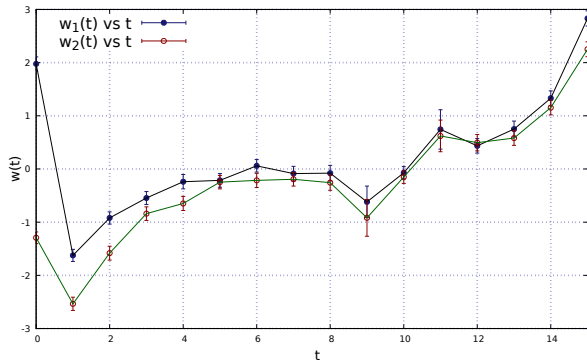
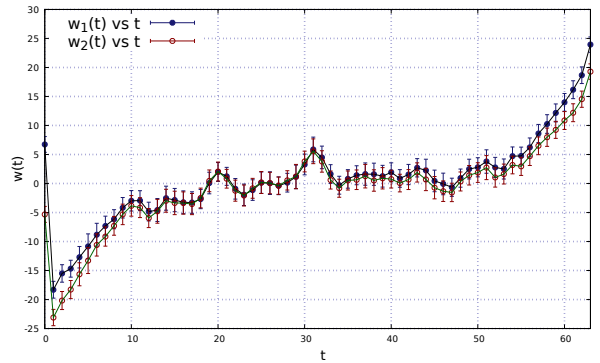


FIG. 6: Mass-gap ratios against  $a$  for degree-five superpotential with parameters  $m = 10$  and  $g = 100$ . In the box the plot of  $m_{\text{phys}}$  against  $a$  is shown. The simulation data indicate that SUSY is broken in this model.



(a) Ward identities on a  $T = 16$  lattice.



(b) Ward identities on a  $T = 64$  lattice.

FIG. 7: Ward identities on  $T = 16$  and  $T = 64$  lattices for parameters  $m = 10$  and  $g = 100$ . The simulation data indicate that SUSY is broken in this model.

$T$	$\langle S \rangle$	$\frac{\langle S \rangle}{T}$
8	7.3378(1056)	0.9172(132)
16	15.3381(1106)	0.9586(69)
32	30.9851(924)	0.9683(29)
64	63.0699(2014)	0.9855(32)

TABLE IV: The expectation values of the action for degree-five superpotential. We used the parameters  $g = 100$  and  $m = 10$  in the simulations. The data suggest that supersymmetry is broken in this model.

The results in Fig. 6 clearly show that the ratio of extracted mass gaps are completely different as  $a \rightarrow 0$ . From Fig. 7 we see that the Ward identities are not satisfied suggesting that SUSY is broken in this model. Another indication of SUSY breaking is that the expectation value of the action is not equal to  $T$ . In Fig. 8 we show the plot of the normalized action against the number of lattice sites. This also indicates that SUSY is broken in this model.

In the next subsection we show the simulation results of the same model with anti-periodic boundary conditions. The simulations again confirm broken SUSY in this model.

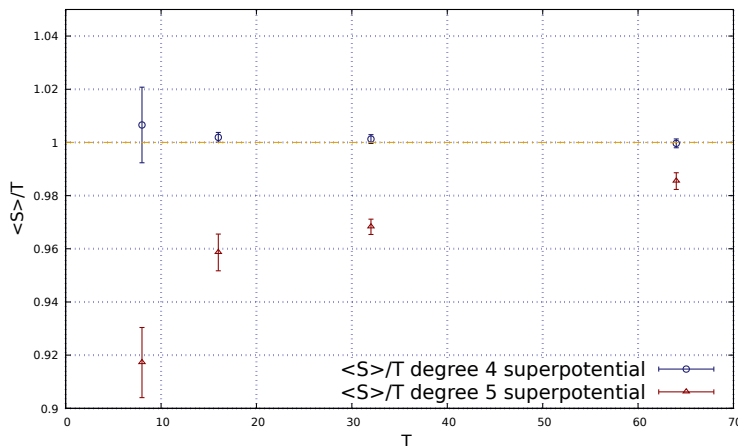


FIG. 8: The normalized action for the model with degree-five superpotential. The parameters used are  $g = 100$  and  $m = 10$ . Periodic boundary conditions were employed on the lattice. The plot indicates that SUSY is broken in this model.

## 2. Anti-periodic Boundary Conditions

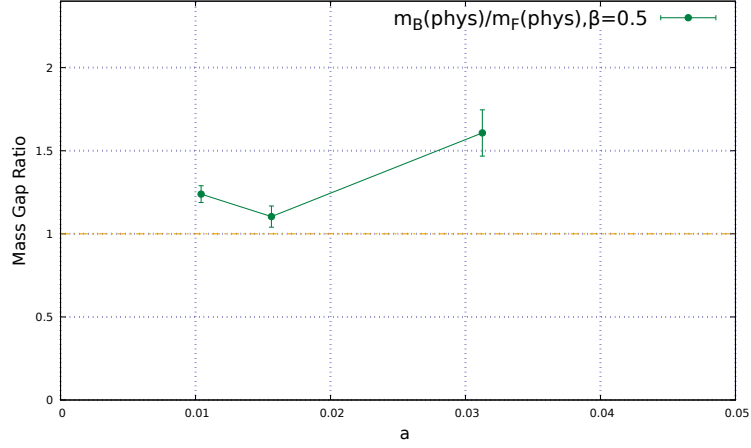
We also studied the model with degree-five superpotential using anti-periodic boundary conditions:  $\psi(T) = -\psi(0)$  and  $\bar{\psi}(T) = -\bar{\psi}(0)$ . The model was simulated on a lattice with  $T = 16, 32$

	$\beta$	$E_0^{(B)\text{phys}} \equiv m_{b(\text{phys})}$	$E_0^{(F)\text{phys}} \equiv m_{f(\text{phys})}$	Mass Ratio = $\frac{m_{b(\text{phys})}}{m_{f(\text{phys})}}$
T = 16	0.5	12.3037(7747)	7.6557(1814)	1.6071(1393)
	1.0	8.1706(6542)	7.1206(2278)	1.1474(1286)
	2.0	6.7611(5851)	6.6794(1479)	1.0122(1100)
T = 32	0.5	10.4122(2963)	9.4349(2874)	1.1036(638)
	1.0	8.7334(4438)	9.4419(2765)	0.9250(741)
	2.0	6.8637(6566)	8.1083(1938)	0.8465(1012)
T = 48	0.5	11.3366(3264)	9.1517(1104)	1.2388(506)
	1.0	12.5928(8462)	7.8192(1378)	1.6105(1366)
	2.0	11.2846(11110)	7.9603(1849)	1.4176(1725)

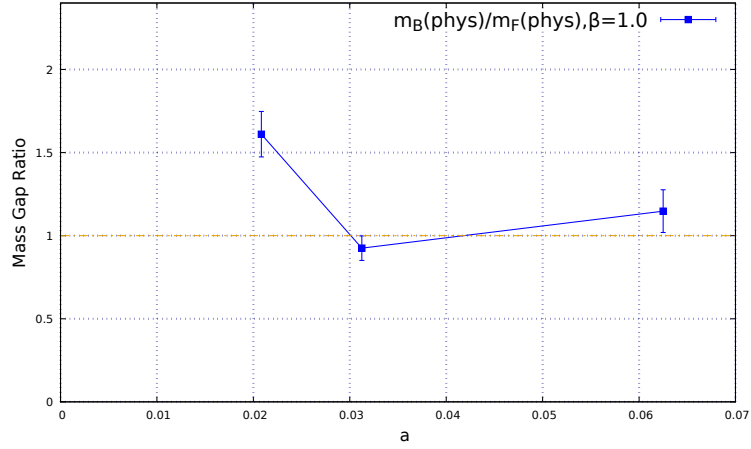
TABLE V: The extracted masses for the model with degree-five superpotential. Anti-periodic boundary conditions are used on the lattice. The parameters used in the simulations are  $g = 100$  and  $m = 10$ . The simulations indicate that SUSY is broken in this model.

and 48 with the inverse temperature  $\beta = aT = 0.5, 1.0, 2.0$ . The mass-gap values extracted from the simulations are given in Table V. For each  $\beta$  we have plotted the mass-gap ratios and they are shown in Fig. 9. It is clear that for all values of  $\beta$ , as  $a$  is decreased, the mass-gap ratio deviates away from 1, which tells us that SUSY is broken in this model.

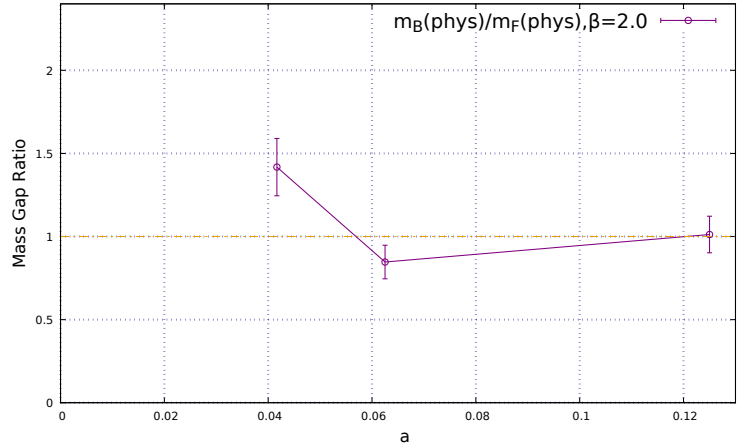
We can also compute the expectation values of the lattice action in all these cases and check if they are equal to  $T$ . The expectation values of the action are given in Table VI. The plot is given in Fig. 10. The data and plot clearly suggest that the expectation values of the action are no longer equal to  $T$ . As  $\beta$  is increased, the SUSY breaking effects become more prominent. These effects are clearly visible in the expectation values of the action and the Ward identities in Fig. 11.



(a)  $\beta = 0.5$ .



(b)  $\beta = 1.0$ .



(c)  $\beta = 2.0$ .

FIG. 9: The extracted mass-gap ratios for various values of  $\beta$  with different number of lattice sites for degree-five superpotential. Anti-periodic boundary conditions were used on the lattice. The simulations indicate that SUSY is broken in this model.

	$\beta$	$\langle S \rangle$	$\frac{\langle S \rangle}{T}$
T = 16	0.5	15.3930(951)	0.9621(59)
	1.0	14.9646(1033)	0.9353(65)
	2.0	14.7355(947)	0.9210(59)
T = 32	0.5	31.2350(0.1632)	0.9761(51)
	1.0	30.7837(0.1704)	0.9620(53)
	2.0	30.1213(1634)	0.9413(51)
T = 48	0.5	47.7246(1758)	0.9943(37)
	1.0	46.7418(1932)	0.9738(40)
	2.0	45.9214(2080)	0.9567(43)

TABLE VI: The expectation values of the action for the model with degree-five superpotential. We used anti-periodic boundary conditions on the lattice. The parameters used in the simulations are  $g = 100$  and  $m = 10$ . The data suggest that SUSY is broken in this model.

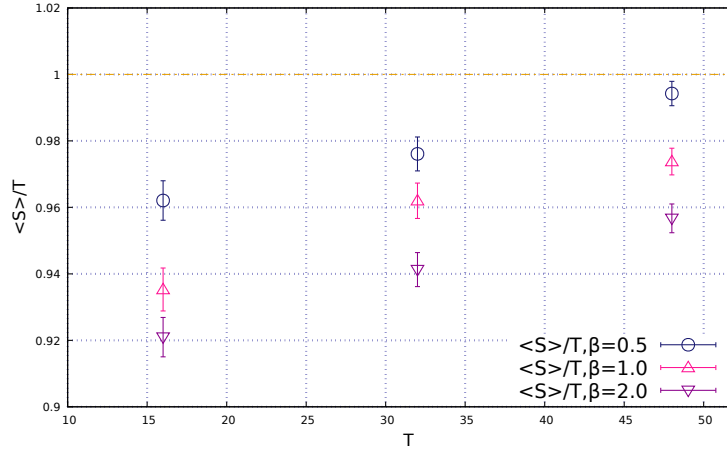
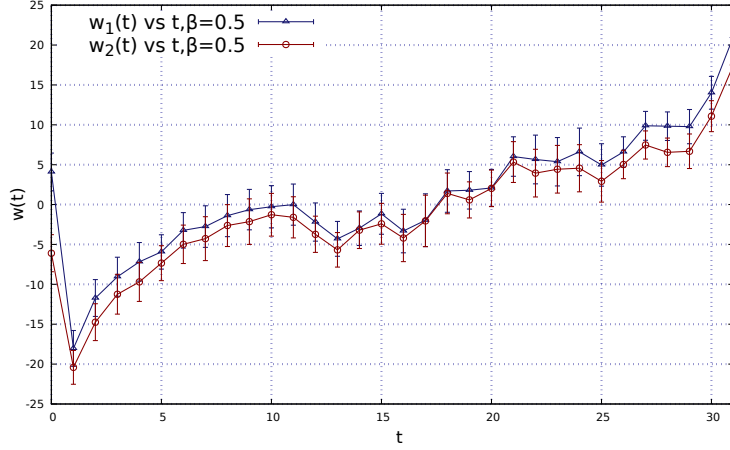
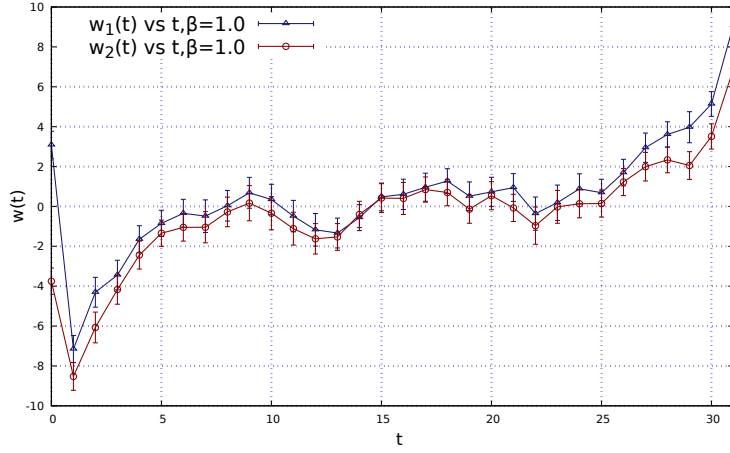


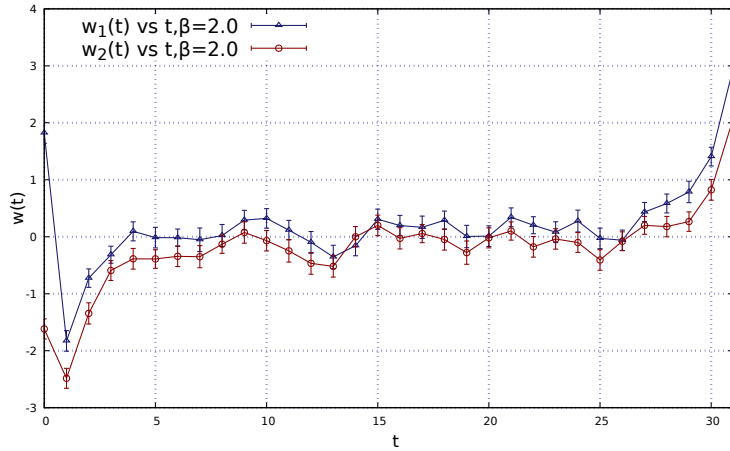
FIG. 10: The expectation values of the action per site against the total number of sites for various  $\beta$  values. The model has degree-five superpotential. Anti-periodic boundary conditions were employed on the lattice. The plot indicates that SUSY is broken in this model. As  $\beta$  is increased the data points are moving away from the horizontal line, which shows the broken nature of SUSY in the zero temperature limit.



(a) For  $\beta = 0.5$ .



(b) For  $\beta = 1.0$ .



(c) For  $\beta = 2.0$ .

FIG. 11: The Ward identities for the model with degree-five superpotential on a  $T = 32$  lattice with  $\beta = 0.5, 1.0$  and  $2.0$ . Anti-periodic boundary conditions were employed on the lattice. The parameters used in the simulations are  $g = 100$  and  $m = 10$ . These plots suggest that SUSY is broken in this model.



### C. Scarf I Superpotential

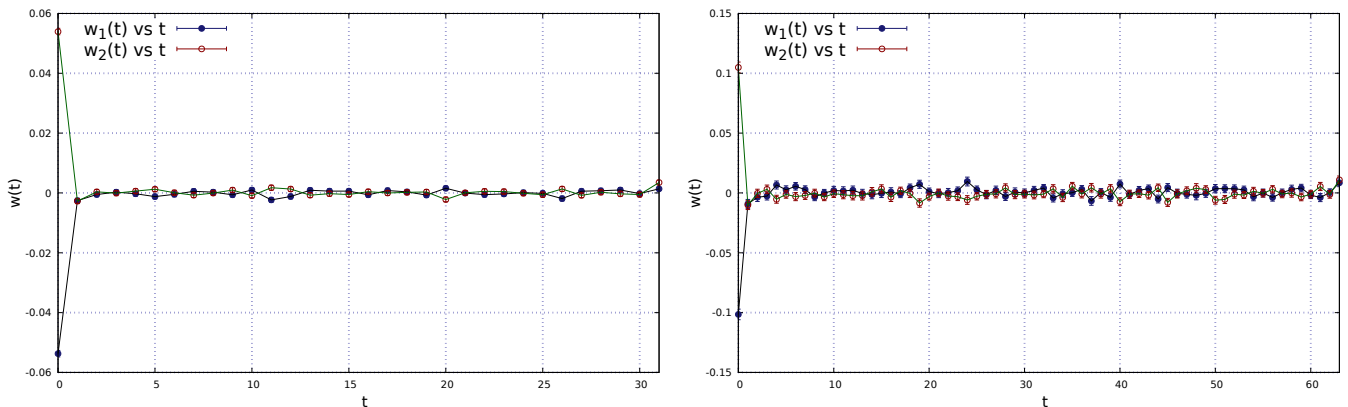
In this section we consider the model with another type of superpotential known as the Scarf I potential. In Ref. [26] it was shown that SUSY is preserved in this model.

We have

$$W'_i = \lambda \alpha \tan(\alpha \phi_i), \quad (3.24)$$

where  $\lambda$  is a dimensionless coupling constant,  $\alpha$  is a parameter with mass dimension  $\frac{1}{2}$ . With this potential, we use the dimensionless parameters,  $\alpha = \alpha_{\text{phys}} a^{1/2}$ ,  $\lambda = \lambda_{\text{phys}}$  and  $\phi = \phi_{\text{phys}} a^{-1/2}$ .

We used the parameters  $\beta = aT = 0.5$ ,  $\alpha = \sqrt{60}$  such that  $\beta\alpha^2 = 30$  for the simulations. The Ward identities for this model are plotted in Fig. 12 for  $T = 32$  and  $64$ . The plots show that the Ward identities are satisfied for  $0 \ll t \ll T$ .



(a) Ward identities on a  $T = 32$  lattice.

(b) Ward identities on a  $T = 64$  lattice.

FIG. 12: The Ward Identities for  $T = 32$  and  $T = 64$  lattices with  $\lambda = 10$  and  $\beta\alpha^2 = 30$  for the model with Scarf I potential. The data show that SUSY is preserved in this model.

### D. Models with $\mathcal{PT}$ -Symmetry

Another class of models we investigated on the lattice is the quantum mechanics with  $\mathcal{PT}$ -symmetric superpotential. Here,  $\mathcal{P}$  and  $\mathcal{T}$  denote the parity symmetry and time reversal invariance, respectively. One of the motivations for considering  $\mathcal{PT}$ -symmetric theories is the following. It is possible to obtain a real and bounded spectrum if we impose  $\mathcal{PT}$ -symmetric boundary conditions on the functional-integral representation of the four-dimensional  $-\lambda\phi^4$  theory [27]. In addition to this, the theory becomes perturbatively renormalizable and asymptotically free. These properties suggest that a  $-\lambda\phi^4$  quantum field theory might be useful in describing the Higgs sector of the Standard Model. It could also play a vital role in the supersymmetric versions of the Standard Model.

In Ref. [28] it was shown that in a two-dimensional supersymmetric field theory, with a  $\mathcal{PT}$ -symmetric superpotential of the form  $W'(\phi) = -ig(i\phi)^{1+\delta}$ , with  $\delta$  a positive parameter, SUSY remains unbroken. A recent study using complex Langevin dynamics showed that SUSY is preserved with these superpotentials [20] in zero-dimensional models. Since Monte Carlo is reliable

only when the action is real, we will be simulating only those  $\mathcal{PT}$ -symmetric superpotentials, which have real actions. For a full analysis of the model with a general  $\delta$  parameter, complex Langevin dynamics or any other compatible method should be employed.

The  $\mathcal{PT}$ -symmetric superpotential has the following form on the lattice

$$W_i = \frac{-g}{2 + \delta} (i\phi_i)^{2+\delta}. \quad (3.25)$$

According to our convention, we use the following derivative of the superpotential

$$W'_i = \sum_j K_{ij} \phi_j - ig (i\phi_i)^{1+\delta}. \quad (3.26)$$

Although we have massless theories as the continuum cousins, we need to introduce Wilson type mass terms for simulations. (See Eq. (3.26).) We perform simulations for various mass values and then take limit  $m \rightarrow 0$ . Since the action needs to be real for Monte Carlo to be reliable, we have worked with  $\delta = 0, 2, 4$ . The superpotentials take the following form for various values of  $\delta$

$$\delta = 0 : \quad W'_i = \phi_i + m\phi_i - \frac{1}{2} (\phi_{i-1} + \phi_{i+1}) + g\phi_i, \quad (3.27)$$

$$\delta = 2 : \quad W'_i = \phi_i + m\phi_i - \frac{1}{2} (\phi_{i-1} + \phi_{i+1}) - g\phi_i^3, \quad (3.28)$$

$$\delta = 4 : \quad W'_i = \phi_i + m\phi_i - \frac{1}{2} (\phi_{i-1} + \phi_{i+1}) + g\phi_i^5. \quad (3.29)$$

In Fig. 13 we show the mass-gap ratio against lattice spacing for a  $\mathcal{PT}$ -symmetric superpotential with  $\delta = 0$  and with parameters  $m = 0$  and  $g = 10$ . In Table VII we show the bosonic and fermionic mass gaps and their ratios for this model. It is clear from the ratios of extracted mass gaps, which is nearly equal to 1, that SUSY is unbroken in this model.

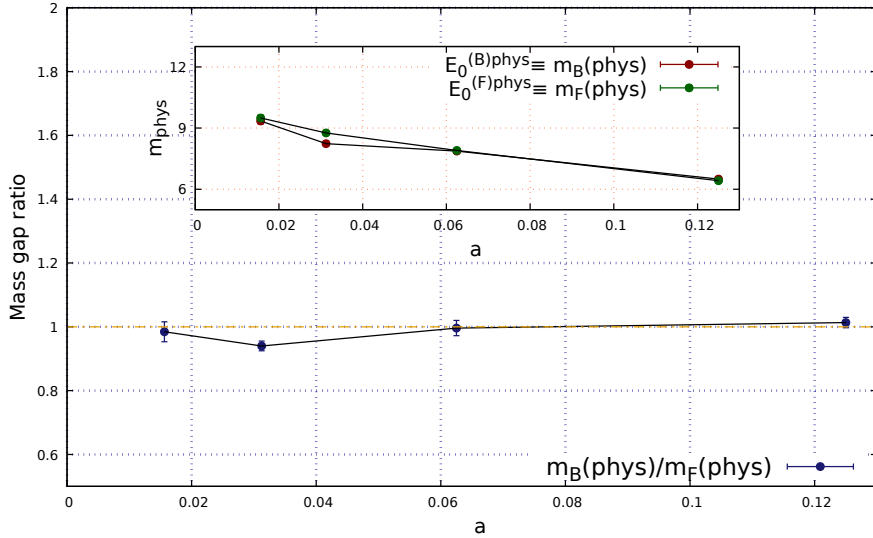


FIG. 13: Mass-gap ratio against  $a$  for the model with  $\mathcal{PT}$ -symmetric superpotential. The parameters used are  $\delta = 0$  and  $g = 10$ . In the box the plot of  $m_{\text{phys}}$  against  $a$  is shown. The simulations indicate that SUSY is preserved in this model.

$T$	$a = T^{-1}$	$E_0^{(B)\text{phys}} \equiv m_{b(\text{phys})}$	$E_0^{(F)\text{phys}} \equiv m_{f(\text{phys})}$	Mass Ratio = $\frac{m_{b(\text{phys})}}{m_{f(\text{phys})}}$
8	0.125	6.5038(706)	6.4191(327)	1.0132(162)
16	0.0625	7.8742(933)	7.9054(962)	0.9961(239)
32	0.03125	8.2384(669)	8.7642(704)	0.9400(152)
64	0.015625	9.3510(1478)	9.4970(1510)	0.9846(312)

TABLE VII: The bosonic and fermionic mass gaps, and their ratios for the model with  $\mathcal{PT}$ -symmetric superpotential. The parameters used are  $\delta = 0$  and  $g = 10$ .

$T$	$a = T^{-1}$	$E_0^{(B)\text{phys}} \equiv m_{b(\text{phys})}$	$E_0^{(F)\text{phys}} \equiv m_{f(\text{phys})}$	Mass Ratio = $\frac{m_{b(\text{phys})}}{m_{f(\text{phys})}}$
8	0.125	4.7488(8471)	4.2192(1923)	1.1255(2521)
16	0.0625	5.2557(14020)	4.2646(4029)	1.2324(4452)
32	0.03125	5.2099(13280)	3.8474(7325)	1.3541(6030)
64	0.015625	0.8123(6495)	1.0878(6491)	0.7467(10426)

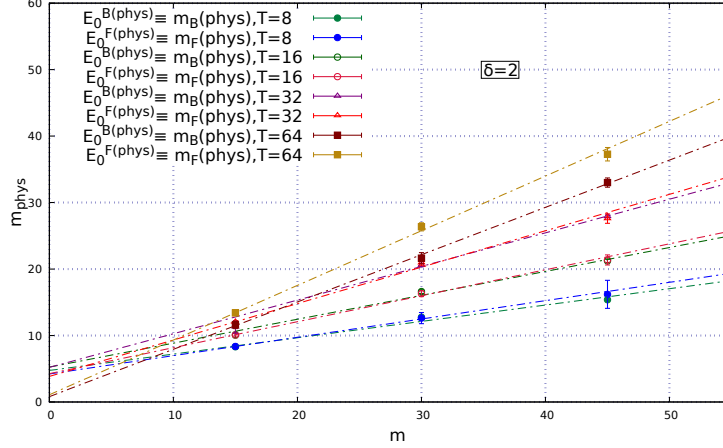
TABLE VIII: The bosonic and fermionic mass gaps, and their ratios for the model with  $\mathcal{PT}$ -symmetric superpotential. The parameters used are  $\delta = 2$  and  $g = 10$ .

For  $\delta = 2$  and 4 we used different values for  $m$  and then extrapolated the results to  $m \rightarrow 0$ . In Fig. 14 (top) we show the  $m_{\text{phys}}$  values extracted from the correlators with different input values of  $m$  for the model with  $\delta = 2$ . The bottom part of the figure shows the mass-gap ratio against  $a$  for  $\delta = 2$ ,  $m = 0$  and  $g = 10$ , and in the box we show the plot of  $m_{\text{phys}}$  against  $a$ . In Fig. 15 we show the similar results for  $\delta = 4$ . The simulation data are provided in Table VIII and Table IX. Again, in both of these cases the extracted mass-gap ratio is nearly 1, suggesting that SUSY is preserved in these models.

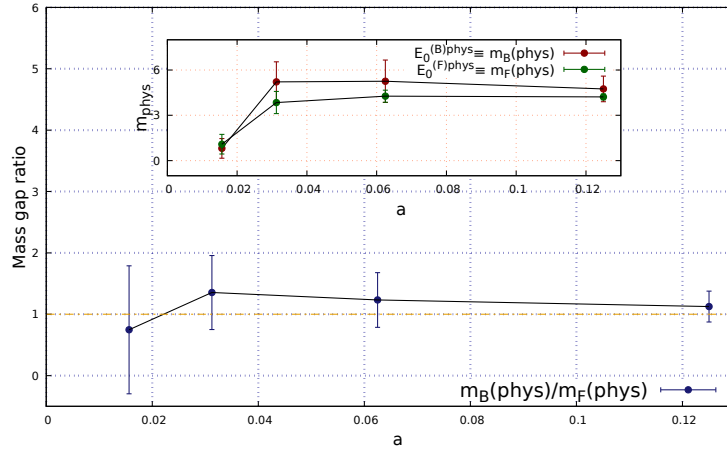
Hence, from the simulation results for  $\delta = 0, 2$  and 4 we see that the extracted values of the bosonic and fermionic mass-gap ratio is 1 within statistical errors. We thus conclude that SUSY is preserved in the case of quantum mechanics models with  $\mathcal{PT}$ -symmetric superpotentials.

$T$	$a = T^{-1}$	$E_0^{(B)\text{phys}} \equiv m_{b(\text{phys})}$	$E_0^{(F)\text{phys}} \equiv m_{f(\text{phys})}$	Mass Ratio = $\frac{m_{b(\text{phys})}}{m_{f(\text{phys})}}$
8	0.125	1.6312(138)	1.7659(319)	0.9237(245)
16	0.0625	1.8791(864)	1.7296(303)	1.0864(690)
32	0.03125	2.1975(560)	1.8979(726)	1.1579(738)
64	0.015625	1.8997(763)	2.2430(2226)	0.8469(1193)

TABLE IX: The bosonic and fermionic mass gaps, and their ratios for the model with  $\mathcal{PT}$ -symmetric superpotential. The parameters used are  $\delta = 4$  and  $g = 10$ .



(a)  $m_{phys}$  extracted from correlators with different input values of  $m$ .

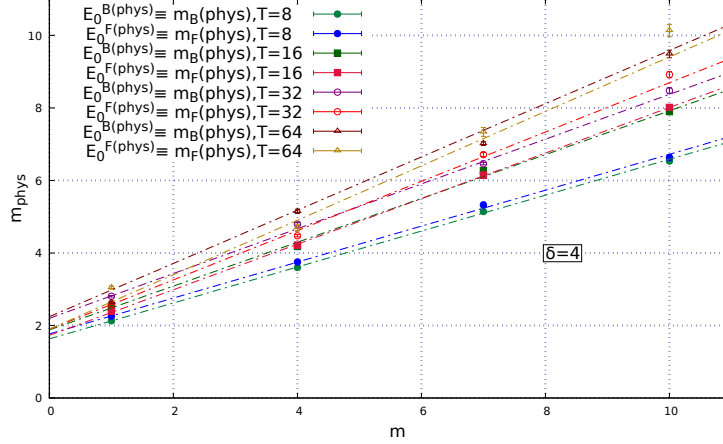


(b) Mass-gap ratio against  $a$  with  $\delta = 2$  and  $g = 10$ . In the box the plot of  $m_{phys}$  against  $a$  is shown.

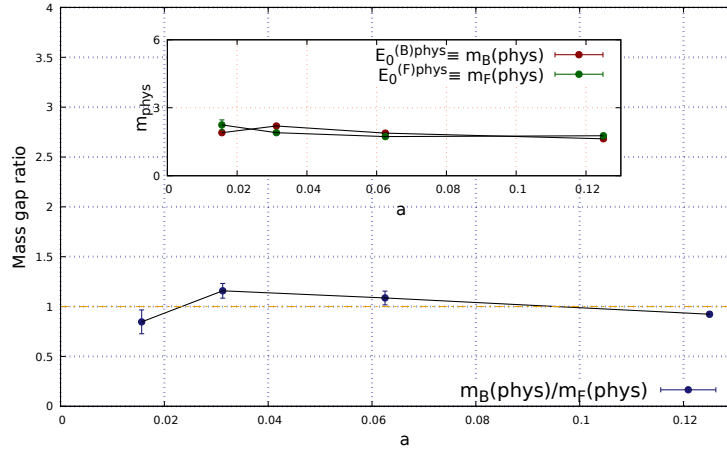
FIG. 14: The bosonic and fermionic mass gaps, and their ratios against  $a$  for the model with  $\mathcal{PT}$ -symmetric superpotential. The parameters used are  $\delta = 2$  and  $g = 10$ .

#### IV. CONCLUSIONS

In this paper, we have investigated non-perturbative SUSY breaking in quantum mechanics models with various types of superpotentials using lattice regularized path integrals. We employed Hamiltonian Monte Carlo (HMC) to perform the field updates on the lattice. After reproducing the results for even and odd polynomial-type superpotentials, we investigated SUSY breaking in Scarf I superpotential. We then moved on to simulate the interesting case of quantum mechanics models with  $\mathcal{PT}$ -symmetry. We simulated these models for various values of the parameter  $\delta$  appearing in the  $\mathcal{PT}$ -symmetric theory, without violating the reliability criteria for Markov chain Monte Carlo simulations. Our simulations indicate that SUSY is unbroken in quantum mechanics models exhibiting  $\mathcal{PT}$  symmetry. An investigation that takes care of arbitrary  $\delta$  values needs a simulation



(a)  $m_{\text{phys}}$  extracted from correlators with different input values of  $m$ .



(b) Mass-gap ratio against  $a$  with  $\delta = 4$ ,  $m = 0$  and  $g = 10$ . In the box the plot of  $m_{\text{phys}}$  against  $a$  is shown.

FIG. 15: The bosonic and fermionic mass gaps, and their ratios against  $a$  for the model with  $\mathcal{PT}$ -symmetric superpotential. The parameters used are  $\delta = 4$  and  $g = 10$ .

algorithm that can handle complex actions such as the complex Langevin method. In Ref. [20] it was shown that  $\mathcal{PT}$  symmetry is preserved in zero-dimensional supersymmetric quantum field theories. Work is in progress to extend these simulations to supersymmetric quantum mechanics with arbitrary  $\delta$  parameter [29]. It would be interesting to reproduce the conclusion given in Ref. [28] using non-perturbative methods such as Monte Carlo method or complex Langevin dynamics. There, it was shown that SUSY remains unbroken, using perturbative calculations, in a two-dimensional supersymmetric field theory, with a  $\mathcal{PT}$ -symmetric superpotential of the form  $W'(\phi) = -ig(i\phi)^{1+\delta}$ , with  $\delta$  a positive parameter. It would also be interesting to perform simulations in four-dimensional supersymmetric models exhibiting  $\mathcal{PT}$  symmetry and thus comment about the nature of the spectrum of the theory.

## V. ACKNOWLEDGEMENTS

We thank discussions with Raghav Jha and Arpith Kumar. The work of AJ was supported in part by the Start-up Research Grant (No. SRG/2019/002035) from the Science and Engineering Research Board (SERB), Government of India, and in part by a Seed Grant from the Indian Institute of Science Education and Research (IISER) Mohali. NSD would like to thank the Council of Scientific and Industrial Research (CSIR), Government of India, for the financial support through a research fellowship (Award No. 09/947(0119)/2019-EMR-I).

### Appendix A: Continuum Theory Calculations

Our action has the following form

$$S = \int d\tau \left( -\frac{1}{2}\phi\partial_\tau^2\phi + \bar{\psi}\partial_\tau\psi - \frac{1}{2}B^2 + \bar{\psi}W''(\phi)\psi - BW'(\phi) \right). \quad (\text{A1})$$

The equation of motion for  $\psi$  and  $\bar{\psi}$  are

$$\partial_\tau\bar{\psi} = W''\bar{\psi}, \quad (\text{A2})$$

$$\partial_\tau\psi = -W''\psi. \quad (\text{A3})$$

The equation of motion for  $B$  is

$$B = -W'. \quad (\text{A4})$$

Putting Eq. (A4) in Eq. (A1) we get the on-shell form of the action

$$S = \int d\tau \left( -\frac{1}{2}\phi\partial_\tau^2\phi + \bar{\psi}\partial_\tau\psi + \bar{\psi}W''(\phi)\psi + \frac{1}{2}(W'(\phi))^2 \right). \quad (\text{A5})$$

The equations of motion stated above are useful in verifying SUSY algebra of supercharges. Let us check the  $Q$  exactness of the action. We have

$$\begin{aligned} QS &= \int d\tau Q \left( -\frac{1}{2}\phi\partial_\tau^2\phi + \bar{\psi}\partial_\tau\psi + \bar{\psi}W''(\phi)\psi + \frac{1}{2}(W'(\phi))^2 \right), \\ &= \int d\tau \left( -\frac{1}{2}\bar{\psi}\partial_\tau^2\phi - \frac{1}{2}\phi\partial_\tau^2\bar{\psi} + \bar{\psi}\partial_\tau(-\partial_\tau\phi + W') + \bar{\psi}W''(-\partial_\tau\phi + W') \right) \\ &\quad + \int d\tau (\bar{\psi}W'''\bar{\psi}\psi + W'W''\bar{\psi}), \\ &= \int d\tau \left( -\frac{3}{2}\bar{\psi}\partial_\tau^2\phi - \frac{1}{2}\phi\partial_\tau^2\bar{\psi} + 2W'W''\bar{\psi} \right). \end{aligned} \quad (\text{A6})$$

Using Eq. (A2) in the last two terms we get

$$QS = \int d\tau \left( -\frac{3}{2}\bar{\psi}\partial_\tau^2\phi - \frac{1}{2}\phi W''\partial_\tau\bar{\psi} - \frac{1}{2}\phi W'''\partial_\tau\phi\bar{\psi} + 2W'(\partial_\tau\bar{\psi}) \right), \quad (\text{A7})$$

where the integration limits are from  $\tau = 0$  to  $\tau = T$ .

Thus we have

$$QS = \left[ -\frac{3}{2}\bar{\psi}\partial_\tau\phi - \frac{1}{2}\phi W''\bar{\psi} - \frac{1}{2}\phi W'''\phi\bar{\psi} + 2W'\bar{\psi} \right]_0^T. \quad (\text{A8})$$

We are also using periodic boundary conditions for the fields

$$\phi(0) = \phi(T), \quad \psi(0) = \psi(T), \quad \bar{\psi}(0) = \bar{\psi}(T). \quad (\text{A9})$$

We note that  $W$  and all its derivatives are functions of  $\phi$ , hence are also the same at the boundaries. Thus all terms in Eq. (A8) vanishes and we get,

$$QS = 0. \quad (\text{A10})$$

Similarly we can show the other transformation on action, i.e.,  $\bar{Q}S = 0$ .

- 
- [1] E. Witten, “Dynamical Breaking of Supersymmetry,” *Nucl. Phys. B* **188** (1981) 513.
  - [2] M. A. Shifman, “Nonperturbative dynamics in supersymmetric gauge theories,” *Prog. Part. Nucl. Phys.* **39** (1997) 1–116, [arXiv:hep-th/9704114](https://arxiv.org/abs/hep-th/9704114).
  - [3] K.-I. Izawa and T. Yanagida, “Dynamical Supersymmetry Breaking in Vector-Like Gauge Theories,” *Progress of Theoretical Physics* **95** no. 4, (04, 1996) 829–830, <https://academic.oup.com/ptp/article-pdf/95/4/829/5228763/95-4-829.pdf>, <https://doi.org/10.1143/PTP.95.829>.
  - [4] Y. Shadmi and Y. Shirman, “Dynamical supersymmetry breaking,” *Reviews of Modern Physics* **72** no. 1, (Jan, 2000) 25–64. <http://dx.doi.org/10.1103/RevModPhys.72.25>.
  - [5] I. Kanamori, F. Sugino, and H. Suzuki, “Observing dynamical supersymmetry breaking with euclidean lattice simulations,” *Prog. Theor. Phys.* **119** (2008) 797–827, [arXiv:0711.2132](https://arxiv.org/abs/0711.2132) [[hep-lat](#)].
  - [6] M. Dine and J. D. Mason, “Supersymmetry and Its Dynamical Breaking,” *Rept. Prog. Phys.* **74** (2011) 056201, [arXiv:1012.2836](https://arxiv.org/abs/1012.2836) [[hep-th](#)].
  - [7] C. Wozar and A. Wipf, “Supersymmetry Breaking in Low Dimensional Models,” *Annals Phys.* **327** (2012) 774–807, [arXiv:1107.3324](https://arxiv.org/abs/1107.3324) [[hep-lat](#)].
  - [8] D. Kadoh and N. Ukita, “General solution of the cyclic Leibniz rule,” *PTEP* **2015** no. 10, (2015) 103B04, [arXiv:1503.06922](https://arxiv.org/abs/1503.06922) [[hep-lat](#)].
  - [9] S. Catterall, R. G. Jha, and A. Joseph, “Nonperturbative study of dynamical SUSY breaking in N=(2,2) Yang-Mills theory,” *Phys. Rev. D* **97** no. 5, (2018) 054504, [arXiv:1801.00012](https://arxiv.org/abs/1801.00012) [[hep-lat](#)].
  - [10] D. Kadoh and K. Nakayama, “Lattice study of supersymmetry breaking in  $N = 2$  supersymmetric quantum mechanics,” *Nucl. Phys. B* **949** (2019) 114783, [arXiv:1812.10642](https://arxiv.org/abs/1812.10642) [[hep-lat](#)].
  - [11] D. Kadoh, T. Kamei, and H. So, “Numerical analyses of  $\mathcal{N} = 2$  supersymmetric quantum mechanics with a cyclic Leibniz rule on a lattice,” *PTEP* **2019** no. 6, (2019) 063B03, [arXiv:1904.09275](https://arxiv.org/abs/1904.09275) [[hep-lat](#)].
  - [12] D. J. F. C., *Trends in Supersymmetric Quantum Mechanics*. Springer International Publishing, Cham, 2019. [https://doi.org/10.1007/978-3-030-20087-9\\_2](https://doi.org/10.1007/978-3-030-20087-9_2).
  - [13] S. Catterall and E. Gregory, “A Lattice path integral for supersymmetric quantum mechanics,” *Phys. Lett. B* **487** (2000) 349–356, [arXiv:hep-lat/0006013](https://arxiv.org/abs/hep-lat/0006013).

- [14] J. Giedt, R. Koniuk, E. Poppitz, and T. Yavin, “Less naive about supersymmetric lattice quantum mechanics,” *JHEP* **12** (2004) 033, [arXiv:hep-lat/0410041](#).
- [15] I. Kanamori, H. Suzuki, and F. Sugino, “Euclidean lattice simulation for dynamical supersymmetry breaking,” *Phys. Rev. D* **77** (2008) 091502, [arXiv:0711.2099 \[hep-lat\]](#).
- [16] G. Bergner, T. Kaestner, S. Uhlmann, and A. Wipf, “Low-dimensional Supersymmetric Lattice Models,” *Annals Phys.* **323** (2008) 946–988, [arXiv:0705.2212 \[hep-lat\]](#).
- [17] S. Schierenberg and F. Bruckmann, “Improved lattice actions for supersymmetric quantum mechanics,” *Phys. Rev. D* **89** no. 1, (2014) 014511, [arXiv:1210.5404 \[hep-lat\]](#).
- [18] D. Baumgartner and U. Wenger, “Supersymmetric quantum mechanics on the lattice: I. Loop formulation,” *Nucl. Phys. B* **894** (2015) 223–253, [arXiv:1412.5393 \[hep-lat\]](#).
- [19] D. Baumgartner and U. Wenger, “Supersymmetric quantum mechanics on the lattice: II. Exact results,” *Nucl. Phys. B* **897** (2015) 39–76, [arXiv:1503.05232 \[hep-lat\]](#).
- [20] A. Joseph and A. Kumar, “Complex Langevin Simulations of Zero-dimensional Supersymmetric Quantum Field Theories,” *Phys. Rev. D* **100** (2019) 074507, [arXiv:1908.04153 \[hep-th\]](#).
- [21] T. Aoyama and Y. Kikukawa, “Overlap formula for the chiral multiplet,” *Phys. Rev. D* **59** (Feb, 1999) 054507. <https://link.aps.org/doi/10.1103/PhysRevD.59.054507>.
- [22] A. Kennedy, “Algorithms for dynamical fermions,” [arXiv:hep-lat/0607038](#).
- [23] J. Sexton and D. Weingarten, “Hamiltonian evolution for the hybrid Monte Carlo algorithm,” *Nucl. Phys. B* **380** (1992) 665–677.
- [24] A. Joseph, “Markov Chain Monte Carlo Methods in Quantum Field Theories: A Modern Primer,” 12, 2019. [arXiv:1912.10997 \[hep-th\]](#).
- [25] S. Catterall and S. Karamov, “Exact lattice supersymmetry: The Two-dimensional N=2 Wess-Zumino model,” *Phys. Rev. D* **65** (2002) 094501, [arXiv:hep-lat/0108024](#).
- [26] D. Kadoh and K. Nakayama, “Direct computational approach to lattice supersymmetric quantum mechanics,” *Nucl. Phys. B* **932** (2018) 278–297, [arXiv:1803.07960 \[hep-lat\]](#).
- [27] C. M. Bender, K. A. Milton, and V. M. Savage, “Solution of schwinger-dyson equations for PT-symmetric quantum field theory,” *Phys. Rev. D* **62** (Sep, 2000) 085001. <https://link.aps.org/doi/10.1103/PhysRevD.62.085001>.
- [28] C. M. Bender and K. A. Milton, “Model of supersymmetric quantum field theory with broken parity symmetry,” *Phys. Rev. D* **57** (Mar, 1998) 3595–3608. <https://link.aps.org/doi/10.1103/PhysRevD.57.3595>.
- [29] A. Joseph and A. Kumar, “Complex Langevin Dynamics and Supersymmetric Quantum Mechanics,” [arXiv:2011.08107 \[hep-lat\]](#).